Deep Rock Foundations of Skyscrapers

L. Ribeiro e Sousa, David Chapman, Tiago Miranda

Abstract. In the case of skyscrapers, the suitable bearing surfaces occur at considerable depth in rock formations, and when it is uneconomical to excavate the overlying weak material, socketed shafts are required for the foundations. In selecting a suitable foundation system, several factors must be taken into consideration. In this article problems associated to deep building foundations in rock formations are explained, as well as the actual evolution of skyscrapers. Geomechanical characterization in terms of deformability and strength of rock masses is analyzed in detail. The design processes of rock-socketed shafts are briefly explained and the foundations of some important buildings in New York and Chicago are presented with the available geotechnical information. Some conclusions on deep rock foundations of skyscrapers are presented.

Keywords: foundations, rock masses, skyscrapers, rock-socketed shafts, design values, settlements.

1. Introduction

The function of a building foundation is to transfer structural loads from a building safely into the ground. The foundation is a critical segment in the construction and performance of a skyscraper; statistics have shown that the most frequent cause of building collapse is an inappropriately built foundation. Therefore, the foundation must be properly designed and constructed. Its stability depends on the behavior of the ground on which it rests under the pressure of structural loads. This is affected by the foundation design and the ground characteristics.

The majority of foundations on rock are spread footings at the ground surface, but in the case of skyscrapers this type of footing may not be suitable. In these situations the suitable bearing surfaces often occur at considerable depths. Removal of the overlying weak material is likely to be uneconomical and socketed shafts are required. In selecting a suitable foundation system for a building, various factors must be taken into consideration including the ground conditions, load transfer pattern, shape and size of the building, site constraints, and the presence of underground structures or environmental issues.

The scope and the purpose of this article are to analyze deep rock foundations of skyscrapers and to provide explanations for caisson foundation design parameters based on general considerations about rock formations. Following this brief Introduction, Section 2 explains different deep rock foundations and evolution of the skyscrapers. Site and geomechanical characterization, in terms of deformability and strength, is analyzed in detail in Section 3. Section 4 shortly explains design processes for rock-socketed shafts and finally, Section 5 analyzes some tall buildings using standard expressions namely regarding settlements. Conclusions are presented in Section 6, as well as acknowledgements and cited references.

2. Evolution of Deep Rock Foundations

2.1. Types of deep foundations

Foundations on rock can be classified into spread footings, socketed shafts and tension foundations. The geotechnical information required for the design of all types of foundations consists of structural geology, geotechnical rock mass properties and ground water conditions (Wyllie, 1999).

Deep rock foundations transfer the load at a point far below the substructure. Deep foundations are used when adequate ground capacity is not available close to the surface and loads must be transferred to firm layers substantially below the ground surface. The common deep foundation systems for buildings are piles and caissons or shafts.

A pile is a column inserted in the ground to transmit the structural loads to a strong soil or rock deep underground. Piles are used in areas where near-surface soil conditions are poor. They are generally made of concrete, steel or a combination of both.

A caisson or shaft is a box or casing filled with concrete and forms a structure similar to a non-displacement pile but larger in diameter. Caisson foundations are used when soil or rock of adequate bearing strength is found below surface layers of weak materials. A caisson is also similar to a column footing in that it spreads the load from a column over a large area of soil so that the allowable stress in the soil is not exceeded. The lower ends of the caissons transfer the building load into the ground (Fig. 1). Ec represents the deformability modulus of the concrete.

There are different types of caissons, namely: i) *Bored* - some soil is removed and a caisson is set into the

L. Ribeiro e Sousa, Professor, Lachel Felice & Associates, P.O. Box 1059, 07962 Morristown, NJ, USA and Civil Engineering Department, University of Porto, Rua Dr. Rodrigo Frias s/n, 4200-465 Porto, Portugal. e-mail: ribeiro.e.sousa@gmail.com.
David Chapman, Engineering Consultant, Lachel Felice & Associates, P.O. Box 1059, 07962 Morristown, NJ, USA. e-mail: dchapman@lachel.com.
Tiago Miranda, Assistant Professor, Geotechnics Group, Civil Engineering Department, University of Minho, Campus of Azurém, 4800-058 Guimarães, Portugal. e-mail: tmiranda@civil.uminho.pt.
Submitted on May 26, 2008; Final Acceptance on December 8, 2008; Discussion open until September 30, 2010.

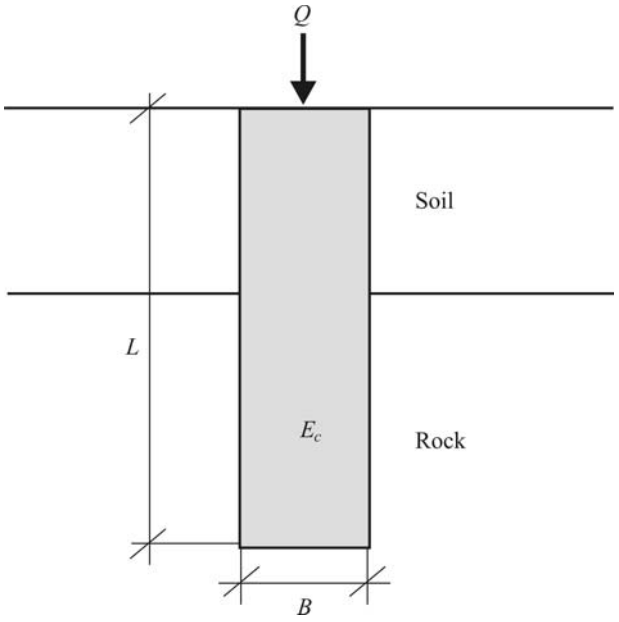

Figure 1 - Caisson or shaft foundation socket into rock.

hole; ii) *Socketed* - a socketed caisson is one that is drilled into rock at the bottom rather than belled; its bearing capacity comes from both its end bearing and frictional forces between the sides of the caisson and the rock; iii) *Box* - a box caisson is a structure with a closed bottom designed to be sunk into prepared foundations below water level; they are unsuitable for sites where erosion can damage the foundations, but they can be placed successfully on natural firm foundation material, on crushed rock placed after dredging soft material, or on a pile foundation; iv) *Pneumatic* - pneumatic caissons are usually used in riverbed work; a concrete box built with an airtight chamber at the bottom is constructed on ground; the air is compressed in the chamber, balancing with the ground water pressure to prevent the ground water from getting into the box and as soil is excavated and removed, the box is gradually sunk into the ground; steel shafts are connected to the pressurized working chamber as access for workers and excavation machinery.

2.2. Evolution of skyscrapers

The worldwide trend is towards living in megacities. It is estimated by 2030 that two thirds of the world population will be urbanized. Therefore a new generation of megacities is predicted to develop in the next twenty years. To accommodate this population the construction of tall buildings is expected to be a major tendency in those megacities (Binder, 2006).

The construction of tall buildings started at the end of the 19th century, particularly in the cities of New York and Chicago. Table 1 presents a list of the buildings that were each considered the tallest building in the world for a some period of time. Until the end of the 1990's all the tallest buildings were constructed in the United States.

Table 1 - Buildings that held the title of the tallest Building in the world (library.thinkquest.org).

Years	Building	Location	Height	Observations
1890-94	NY World Building	New York	94 m	Demolished 1955
1892-94	Masonic Temple	Chicago	92 m	Demolished 1939
1894-99	Manhattan Life Insurance Building	New York	106 m	Demolished 1930
1899-08	Park Row Building	New York	119 m	3,900 piles driven to sand and granite. 29 stories
1908-09	Singer Building	New York	187 m	Demolished 1968
1909-13	Metropolitan Life Insurance Company	New York	213 m	-
1913-30	Woolworth Building	New York	241 m	-
1930	40 Wall Street	New York	283 m	70 storey skyscraper
1930-31	Chrysler Building	New York	319 m	-
1931-72	Empire State Building	New York	381 m to roof	102 storey skyscraper
1972-73	World Trade Center (Twin Towers)	New York	417 m to roof	Designed with columns grouped around the perimeter and within core
1972-98	Sears Tower	Chicago	442 m to roof	-
1998-04	Petronas Twin Towers	Kuala Lum-pur	403 m to roof	The foundations are the deepest in the world
2004-08	Taipei Financial Centre	Taipei	509 m to top	Foundations with deepest dolomite bedrock
2008-	Burj Dubai	Dubai	800 m+	Underway

Nowadays the top four tallest buildings are lead by the tall skyscraper in Taiwan's capital followed by the twin Petronas Towers in Kuala Lumpur, Malaysia. The alignment also shows Chicago's Sears Tower in third place, with Shanghai's Tower in fourth as it is shown in Fig. 2.

The Taipei 101 tower has 101 stories above ground and five underground. Details of the foundation are shown in Fig. 3. The rock formations are dolomites. The building holds several records, namely the distance from the ground to the structural top (509 m), the ground to the roof (449 m) and the fastest ascending elevator speed. However the longest distance from ground to antenna is still held by Sears Tower with 527 m.

The Petronas Twin towers are the tallest twin towers in the world, owned by Malaysia's national oil company. They are supported by deep foundations of varying lengths consisting of rectangular cast-in places piles that extend to 130 m below grade with ground improvement up to 162 m depth. The challenges of the foundation were to be built on karstic bedrock (DFI, 2008).

However, several spectacular new buildings are planned for construction in the near future as shown in Table 2.

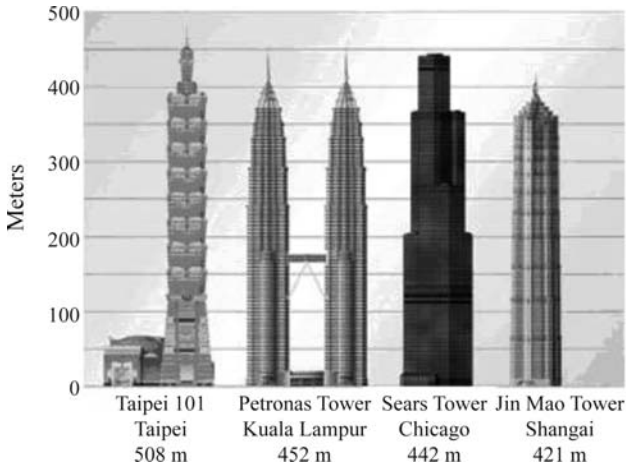

Figure 2 - Worlds top four tallest buildings (library.thinkquest.org).

The Palm tower also designated by Al Burj tower, a proposed skyscraper in Dubai, United Arab Emirates, will stand as the highest with about 643 m high to roof, and 808 m to antenna (Fig. 4). The site for the tower is an offshore island, which posed an unusual challenge to building. The Al Burj tower is built in reinforced concrete and is very slender in form. The 160-story tower has a hotel in the base, apartments from the 20th to the 110th story and offices above. The foundation evaluation was complicated by highly variable weak rock and high design loads. The designer developed an Osterberg load test program, testing several combinations of barrettes and bored piles from 50 to 75 m in depth (STS, 2006).

However, there are big changes coming in rankings. In the CBTUH Conference held in 2008, in its view of

Figure 3 - Dolomite foundations of Taipei 101 tower (STS, 2006).

Table 2 - Tallest buildings in the near future.

Year of completion	Building	Location	Height	Observations
2009	Freedman Tower	New York	417 m to roof; 541 m to antenna	-
2009	Burj Dubai	Dubai	643 m to roof; 808 m to antenna	Foundation with 192 piles descending to a depth of more 50 m
2009	Trump Int. Hotel & Tower	Chicago	-	Bearing capacity of 25.9 MPa
2009	China Building TV Tower	Guan-gzhou	610 m	The base footprint is triangular
2011	Chicago Spire	Chicago	610 m to roof	Bearing capacity of 28.7 MPa
2012	Moscow Tower	Moscow	612 m	130-story tower

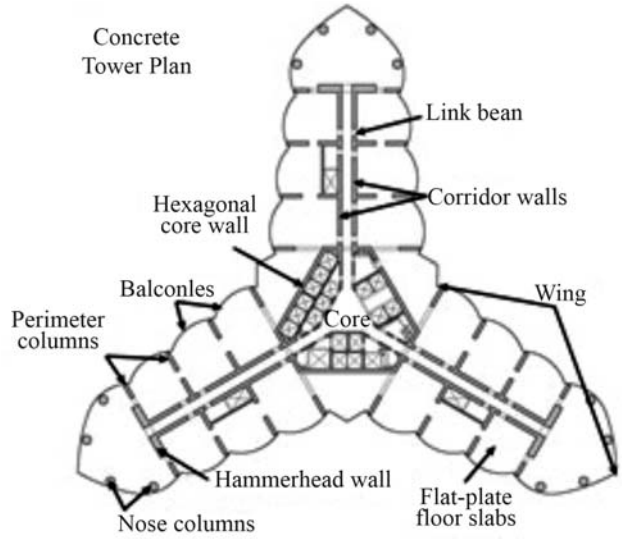

Figure 4 - Concrete tower plan of Al Burj tower (Reina, 2006a).

Figure 5 - Location of Chicago Spire near the lake (Hampton, 2007).

2020, there are proposals of 1,050 m Al Burj in Dubai and 1,001 m Burj Mubarak al-Kabir in Subiya, Kuwait (Post, 2008a, b).

In the Middle East, numerous skyscrapers are under construction as shown in Table 3. At the end of 1999, the 321 m Burj Al Arab, in Dubai, became the world's tallest hotel and in 2000; the Emirates Tower, also in Dubai, was finished, a twin-tower project composed of a 355 m office tower and a 309 m hotel (Binder, 2006).

In the USA special mention is made of the Chicago Spire which will be a 610 m tall twisting spire designed by architect-engineer Santiago Calatrava. The splendid spire, to overlook Lake Michigan, would easily top the 442 m high Sears tower as the US tallest building. Figs. 5 and 6 give images of the proposed tower. The building is located at Lake Shore Drive and the groundbreaking was on June 25, 2007. The predicted completion is in the year 2011 and the building will provide a floor area of about 278,700 m^2 (Hampton, 2007).

Calatrava's latest concept in skyscrapers is an all-concrete building of square-shaped floors that stack onto each other in two-degree horizontal offsets. The finished effect is an approximately 488 m tall structure that twists 360° from bottom to top. Each floor would have four concave sides and cantilevered corners. A tapering concrete core would resist wind and gravity loads, while 12 shear walls radiating from the core would provide additional support. The tower is composed by 300 condos and placed in the top a luxury hotel (Hampton, 2007).

After the tragedy of September 11, 2001, an imaginative outcropping of design has emerged in order to rebuild the World Trade Centre site in New York.

The official proposal comprehends 7 tall buildings. The Freedom tower designed by Norman Foster & Partners will be the most impressive. Figure 7 shows an image of the tower to be finished in 2009. The building heights are 417 m to the roof and 541 m to the antenna. It has a sloping roof on a 70-story building, and an open-air superstructure, windmills and suspension cables (Stephens, 2004).

Table 3 - Tallest buildings in the Middle East.

Name	City	Country	Year	Storys	Height (m)
Burj Dubai	Dubai	UAE	2009	150+	700+
Abraj Al Bait	Makkah	Saudi Arabia	2008	76	485
Burj Al Alam	Dubai	UAE	2009	108	484
Dubai Towers	Doha	Qatar	2008	86	445
Princess Tower	Dubai	UAE	2009	102	414
Al Hamra Tower	Kuwait City	Kuwait	2009	77	412
23 Marina	Dubai	UAE	2008	90	389
Najd Tower	Dubai	UAE	2008	82	375
The Torch	Dubai	UAE	2008	80	345

In Europe, the first skyscraper was built at Antwerp, Belgium, in 1932: the 26-storey Torengebouw that remained until the 1950s. Until the early 1970s, many high buildings in Europe were hotels. Moscow's 34 storey Ukraina hotel constructed in 1957 remains Europe's tallest hotel. Nowadays, Europe is not known as a tall buildings zone, however some important tall buildings have been constructed as referred in the publication of Binder (2006).

Figure 6 - Detailed view of Chicago Spire (DFI, 2008).

Figure 7 - Location of Freedom tower (Stephens, 2004).

In Moscow, several impressive tall buildings are under construction. Special reference is made to the proposed 520,800 m^2 Moscow Tower, sited a few kilometers from Red Square, which would provide office, residential and conference space. This skyscraper in Moscow will be potentially the Europe's tallest building. It was designed by Norman Foster & Partners. The building is a 130-story tower and its basement will be over 30 m deep in alternating clay and limestones.

3. Site and Geomechanical Characterization

3.1. General

Due to the variability of rock formations, the evaluation of geotechnical properties is one of the issues with the largest degree of uncertainty. This fact is a consequence of the complex geological processes involved and to the inherent difficulties of geomechanical characterization (ASCE, 1996; Sousa *et al.*, 1997; Miranda, 2003). The evaluation of the geomechanical parameters is mainly carried out through *in situ* and laboratory tests and also by the application of empirical methodologies (Bieniawski, 1989; Barton, 2000; Hoek, 2006).

In situ tests for the deformability characterization are normally carried out by applying a load in a certain way and measuring the correspondent deformations of the rock mass. Shear and sliding tests for strength characterization are normally performed in low strength surfaces. These strength tests are expensive and the strength parameters evaluation of the rock mass is normally carried out indirectly by the Hoek and Brown (H-B) strength criteria normally associated with the GSI empirical system.

Laboratory tests affect only a small rock volume and consequently it is necessary to perform a considerable number of tests in the rock and in the discontinuities in order to characterize the variability of the determined geomechanical parameters. Laboratory tests such as the determination of uniaxial compressive strength (UCS), point-load and discontinuities tests are also very important for the empirical methodologies.

Based on experience, it can be said that it is necessary to obtain direct geomechanical information from the site and it is not adequate to extrapolate from other situations. Only generic considerations can be made in order to obtain answers to the problem of deep foundations without site-specific geomechanical information.

However, the knowledge of the intact rock properties is always important. Some results obtained from a compilation of rock properties performed by Judd (1969) are presented in Table 4.

One of the goals of the study conducted by Judd (1969) was to establish rock property values that can be correlated with an acceptable correlation coefficient, and then minimize the types of tests required for design and construction of engineering structures.

The study indicated that there appears to be some usable degree of linear correlations between the rock properties determined by dynamic loads and its unconfined compressive strength, and with elastic properties measured by static load tests and its impact toughness.

Table 4 - Rock properties obtained from Judd (1969).

Rock	Properties	Values		
		Mean	Max.	Min.
Dolomite	Mod. def. (GPa)	29.0	73.6	2.1
	UCS (MPa)	214	365	20
	Permeab. (see 1)	1	2	1
	Poisson ratio	0.12	0.25	0.01
Basalt	Mod. def. (GPa)	38.8	75.9	1.7
	UCS (MPa)	23.4	45.5	2.1
	Permeab. (see 1)	2	3	1
	Poisson ratio	0.16	0.42	0.01
Breccia	Mod. def. (GPa)	12.3	17.7	5.4
	UCS (MPa)	11.0	29.3	0.8
Diorite	Mod. def. (GPa)	69.7	106.7	33.8
	UCS (MPa)	203.4	333.1	84.1
	Permeab. (see 1)	1	1	1
	Poisson ratio	0.25	0.32	0.15
Gneiss	Mod. def. (GPa)	51.4	103.4	7.2
	UCS (MPa)	178.6	304.8	35.9
	Permeab. (see 1)	1	2	1
	Poisson ratio	0.21	0.35	0.10
Granite	Mod. def. (GPa)	28.3	79.4	0.3
	UCS (MPa)	161.4	353.1	35.2
	Permeab. (see 1)	1	2	1
	Poisson ratio	0.16	0.26	0.05
Limes-tone	Mod. def. (GPa)	38.4	81.4	0.1
	UCS (MPa)	75.2	260.7	1.4
	Permeab. (see 1)	2	4	1
	Poisson ratio	0.22	0.48	0.01
Sand-stone	Mod. def. (GPa)	7.1	90.3	0.1
	UCS (MPa)	62.7	328.3	2.1
	Permeab. (see 1)	3	4	1
	Poisson ratio	0.12	0.50	0.01

(1) 1 = 0.001-1 x 10^{-8} m/s; 2 = 1-100 x 10^{-8} m/s; 3 = 100-100,000 x 10^{-8} m/s; 4 > 100,000 x 10^{-8} m/s.

Typical *in situ* load-deformation behavior of the rock mass is completely different from that observed in laboratory tests, mainly due to the presence of discontinuities in the rock mass. Rock masses exhibits characteristics of the rock material and discontinuities, which tend to make the deformability and strength properties of the rock foundations highly direction dependent (Kulhawy & Goodman, 1987).

To characterize rock masses for major building foundations, extensive and specialized exploration programs have to be conducted. They consist normally of vertical borings or even large-diameter shafts which allow a direct examination of the sidewalls and provide access for obtaining high-quality undisturbed samples. Extensive laboratory testing is done and *in situ* testing is carried out to measure the strength and deformability properties of the rock mass (Kulhawy and Carter, 1992a; ASCE, 1996; Sousa *et al.*, 1997).

3.2. Deformability properties

The mechanical characterization of the rock masses formations can be carried out through representative amounts of *in situ* tests. They are in general expensive and subject to significant uncertainties. A good site characterization together with the use of empirical methodologies should be used in the assessment of the design values for geomechanical parameters.

The characterization is also made through laboratory tests on the intact rock and on the discontinuities. The main question is related to their representativeness due to the small volume involved in the tests. Table 5 gives a summary of the primary *in situ* and laboratory tests of rock formations and intact rocks (Rocha, 1971; Baguelin *et al.*, 1978; ASCE, 1996).

Considering the evaluation of the deformability parameters, *in situ* tests can involve small volumes as in the case of the dilatometers or pressuremeters, or large volumes as in case of Large Flat Jacks (LFJ) tests or Plate Load Tests (PLT). Figure 8 presents approximate values of the involved volumes reporting experience in several projects.

In situ tests performed inside a borehole involve small volumes of the rock masses and they can be grouped in two main types, depending on the way the pressure is applied to the walls of the borehole (Baguelin *et al.*, 1978; Sousa *et al.*, 1997):

• Application of pressure through a flexible membrane adapted to the walls of the hole with an axyssimetrical pressure. Using dilatometers, as it is the case of the BHD dilatometer used in Portugal, radial deformations are measured while for the pressuremeter a volumetric deformation is measured. The last is more suitable to be used in soft rocks.

• Application of the pressure through rigid plates in two circumferential arches, which corresponds to a more complex load situation and consequently has more associ-

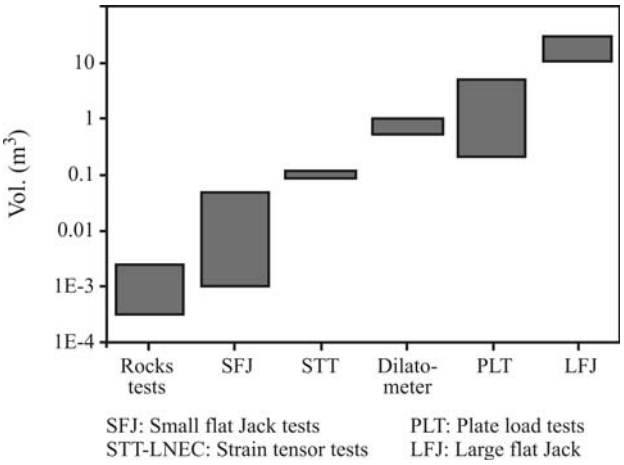

Figure 8 - Approximate volumes involved for different tests (Miranda, 2007).

ated interpretation challenges, as it is the case of Goodman jack dilatometer.

In situ tests in a gallery or at the surface can involve larger volumes, being therefore more representative. Not considering radial load tests and biaxial or triaxial *in situ* tests, the primary *in situ* tests are the following:

• PLT – the load is applied by means of a jack and the rock displacements are measured at the surface or in boreholes behind each loaded area.

• LFJ tests – the load is applied in the walls of one or more opened slots. There are also the SFJ tests that involve a smaller area but allow in addition determining the *in situ* stress state components.

• Seismic tests between boreholes and galleries – these tests allow determining the dynamic modulus measuring S and P wave's velocities. The values obtained are different from the static ones due to difference in time and deformation level applied during the tests. They can involve considerable volumes and can be correlated with the static tests results.

There are no universal rules to define which tests should be carried out for a given situation since each test presents advantages and drawbacks. A good plan should rely on engineering experience and the particular project issues. For rock masses presenting high anisotropy levels, tests should be carried out in order to define the parameters that characterize that anisotropy. This can be carried out by computing indexes which relate rock properties (for instance the uniaxial compressive and point load strengths and longitudinal wave velocity) perpendicular and parallel to planes of anisotropy.

In order to quantify the rock mass deformability the number of *in situ* tests should be rationalized. Excluding the situation of important faults involved, a methodology combining a small number of large scale tests with a larger number of small scale tests should be adopted (Sousa *et al.*, 1997):

Table 5 - *In situ* and laboratory tests for Rock Mechanics (adapted from ASCE, 1996).

Purpose of tests	*In situ* tests	Laboratory tests
Deformability	Geophysical (refraction) Dilatometer/ pressuremeter LFJ and SFJ PLT Borehole jacking Chamber pressure	Uniaxial compression Triaxial compression Swelling Creep
Strength	Direct shear Rock pressuremeter Uniaxial compression Borehole jacking	Uniaxial compression Direct shear Triaxial compression Direct tension Brazilian Point load
Permeability	Constant head Falling head Well pumping Pressure injection	Gas permeability Water content Porosity Absorption
Stress conditions	Hydraulic fracturing Overcoring SFJ Pressuremeter-dilatometer	Overcoring biaxial Overcoring triaxial
Others	Anchor-rockbolt loading	Unit weight Rebound Sonic waves Abrasion resistance

• Zoning of the rock mass considering the available geotechnical information and the use of empirical systems.

• For each zone, small scale *in situ* tests should be executed in boreholes or galleries. They should be in sufficient number in order to assure a good characterization of the rock mass. The location of the tests can be chosen randomly in order to obtain a representative mean value of the deformability modulus or in zones in which lower values are expected.

• For each zone, *in situ* large scale tests can be executed in a smaller number. The results should be calibrated with the values obtained in the small scale tests. Depending on the deformability values, three different situations can be considered, as indicated in Table 6.

Empirical classification systems are also used for the purpose of deformability characterization of rock masses.

Table 6 - Evaluation of large scale tests needs.

Situation	E (GPa)	Large scale tests
I	$E \geq 10$	Advisable
II	$5 \leq E < 10$	Necessary
III	$0.1 \leq E < 5$	Necessary with high precision

Several proposals have been made in the literature (Miranda, 2007). The systems present several drawbacks and intrinsic limitations that should be known by the design engineers for their correct use. The empirical systems with wider application for the preliminary calculation of geomechanical parameters are the RMR, Q and GSI systems. Table 7 presents some of the more representative analytical expressions developed by several authors, as well as their limitations and references.

Also, Data Mining (DM) techniques can be applied in order to obtain new models for geomechanical characterization. A methodology was developed and applied to the granite rock mass formations of the Venda Nova II underground hydroelectric scheme (Lima *et al.*, 2002). The available data was mainly obtained through the application of the most widely used empirical systems and from the results traditional laboratory and *in situ* tests (LFJ, SFJ and dilatometers). Concerning the empirical classification systems applications, and for the underground powerhouse complex, data was organized in a database composed of 1230 examples and with 22 attributes. Several new models were established for these homogeneous granite formations (Miranda, 2007).

The developed models were updated with information obtained through large scale tests (LFJ tests) in a generic Bayesian framework, and finally through the observed behavior of the underground structures during construction (Miranda, 2007; Miranda *et al.*, 2008).

In many cases, the displacements of rock foundations control the design. Several models have been established for foundations on rock assuming the idealization of the discontinuous rock mass as an isotropic or anisotropic elastic continuum (Kulhawy and Carter, 1992b; Yufin *et al.*, 2007).

For these models, and for engineering purposes, it is useful to define a modulus reduction factor α, which represents the ratio of deformability modulus between rock mass and a smaller element of the rock material. Figure 9 represents the modulus reduction factor *vs.* the RMR coefficient. The correlation is based on values referenced in Bieniawski (1975), regarding foundations of dams, bridges, tunnels and power plants, and experimental results from the Venda Nova II hydroelectric scheme (Lima *et al.*, 2002; Placencia, 2003; Miranda, 2007), the Miranda II hydroelectric scheme (Sousa *et al.*, 1999), the Porto Metro (Miranda, 2003) and the Socorridos hydroelectric scheme (Cafofo, 2006) were added.

The curve that better fits the experimental results is represented by the Eq. (1):

$$\alpha = 0.083\, e^{[0.0269\, RMR]} \quad (1)$$

3.3. Strength properties

For the determination of the rock mass strength parameters, large scale *in situ* and laboratory tests for the intact rock and discontinuities can be executed. The main *in situ* tests are: sliding or shearing on discontinuities, in the fault filling materials and along other low strength surfaces and at the rock mass/concrete interfaces. The primary laboratory tests for intact rock strength evaluation are (Rocha, 1971; ASCE, 1996): uniaxial compression, triaxial, diametral linear (Brazilian test), point load, uniaxial tension, shear and tension (Table 5).

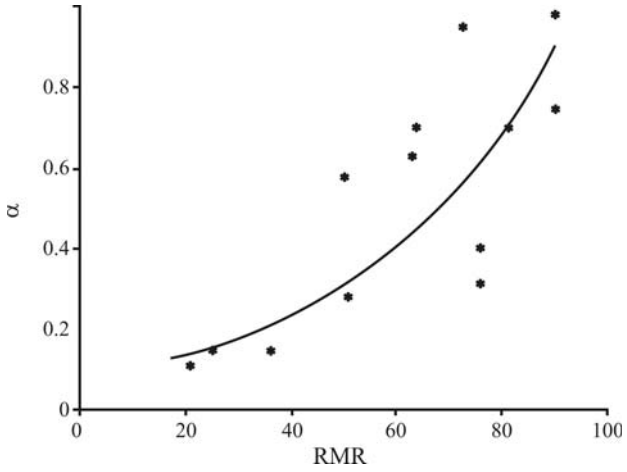

Figure 9 - Modulus reduction factor *vs.* RMR.

In this context the use of empirical systems represents an important tool for the prediction of strength parameters for a given failure criterion. The GSI (Geological Strength Index) system was specially developed to obtain rock mass strength parameters (Hoek, 2006). The system uses the qualitative description of two fundamental parameters of the rock mass: its structure, and the condition of its discontinuities. This system has also been used for evaluation of heterogeneous rock masses in Porto Metro and tunnels in Greece and other difficult rock mass conditions like flysch (Marinos & Hoek, 2005; Babendererde *et al.*, 2006).

Normally, the calculation of the GSI value is based on correlations with modified forms of the RMR and Q indexes, taking into consideration the influence of groundwater and orientation of discontinuities (Hoek, 2006). Other approaches, defined by several authors, can be used for the GSI evaluation (Miranda, 2007).

Based on experimental data and theoretical knowledge of fracture mechanics, the H-B criterion for rock masses is translated by:

$$\sigma'_1 = \sigma'_3 + \sigma_c \left(m_b \frac{\sigma_3}{\sigma_c} + s \right)^a \quad (2)$$

where σ'_1 and σ'_3 are, respectively, the maximum and minimum effective principal stresses, m_b a reduced value of the m_i parameter which is a constant of the intact rock, and s and a are parameters that depend on characteristics of the rock formation. Serrano *et al.* (2007) extended this failure

Table 7 - Analytical expressions for the calculation of E based in empirical systems (adapted from Miranda, 2007).

System	Expression	Limitations	Reference
RMR	E (GPa) = $10^{(RMR\ -\ 10)/40}$	$RMR \leq 80$	Serafim & Pereira (1983)
	E (GPa) = $2RMR$ - 100	$RMR \geq 50 \wedge \sigma_c \geq 100$ MPa	Bieniawski (1978)
	$E(\text{GPa}) = \frac{\sqrt{\sigma_c}}{10} 10^{(RMR-10)/40}$	$\sigma_c \leq 100$ MPa	Hoek & Brown (1997)
	E (GPa) = $0.3H^{\alpha}$ $10(RMR$ - $20)/38$	$\sigma_c > 100$ Mpa $\wedge$ $H > 50$ m	Verman (1993)
	$E = E_i/100 \times\ 0.0028RMR^2 + 0.9e^{(RMR/22.28)}$	-	Nicholson & Bieniawski (1997)
	$E/E_i = 0.5 \times\ (1 - \cos(\pi \times RMR/100))$	-	Mitri *et al.* (1994)
	E (GPa) = $0.1 \times (RMR/10)^3$	-	Read *et al.* (1999)
Q	E (GPa) = $25 \times \log Q$	$Q \geq 1$	Barton *et al.* (1980)
	E (GPa) = $10 \times Q_c^{1/3}$; $Q_c = Q\sigma_c/100$	$Q \leq 1$	Barton & Quadros (2002)
	E (GPa) = $H^{0.2} \times Q^{0.36}$	$H \geq 50$ m	Singh (1997)
	$E(\text{GPa}) = 7 \pm 3\sqrt{Q'}$	-	Diederichs & Kaiser (1999)
GSI	$E(\text{GPa}) = (1 - D/2)\frac{\sqrt{\sigma_c}}{10} 10^{(GSI-10)/40}$	$\sigma_c \leq 100$ MPa	Hoek *et al.* (2002)
	E (GPa) = $(1 - D/2)$ $10^{(GST\ -\ 10)/40}$	$\sigma_c \geq 100$ MPa	Hoek *et al.* (2002)
	$E(\text{GPa}) = E_i\left(\frac{1 - D/2}{1 + \exp((60 + 15D - GSI)/11)}\right)$	-	Hoek & Diederichs (2006)
	$E(\text{GPa}) = 100000\left(\frac{1 - D/2}{1 + \exp((60 + 15D - GSI)/11)}\right)$	-	Hoek & Diederichs (2006)
	E (GPa) = $E_i\, s^{1/4}$	-	Carvalho (2004)
	E (GPa) = $E_i\, (s^{\alpha})^{0.4}$	-	Sonmez *et al.* (2004)

α varies between 0.16 and 0.30 (higher for poorer rock masses); H is depth.

criterion to 3D in order to consider the intermediate principal stress in the failure strength of rock masses.

The H-B criterion has some limitations that should be taken into account and some developments have been introduced (Douglas, 2002; Carter *et al.*, 2007; Carvalho *et al.*, 2007).

Once the value of GSI is determined, the parameters of the H-B criterion can be calculated through the following equations:

$$m_b = m_i \exp\left(\frac{GSI - 100}{28 - 14D}\right)$$
$$s = \exp\left(\frac{GSI - 100}{9 - 3D}\right) \qquad (3)$$
$$a = \frac{1}{2} + \frac{1}{6}\left(\frac{GSI - 100}{9 - 3D}\right)$$

where D is a parameter developed for the underground works of the Porto Metro that depends on the disturbance to which the rock mass formation was subjected due to blasting and stress relaxation (Hoek *et al.*, 2002). For $GSI > 25$, m_b can also be calculated through the expression:

$$m_b = m_i s^{1/3} \qquad (4)$$

For many cases of foundations on rock and for certain geotechnical software, it is convenient to use the equivalent cohesion (c') and friction angle (φ') to the H-B criterion parameters. The range of stresses should be within $\sigma_{t,mass} < \sigma_3 \leq \sigma'_{3max}$. The value σ'_{3max} should be determined for each specific case:

$$\frac{\sigma'_{3\,\max}}{\sigma'_{cm}} = 0.47\left(\frac{\sigma'_{cm}}{\gamma H}\right)^{-0.94} \qquad (5)$$

where σ'_{cm} is the rock mass strength, γ is the volume weight and H the depth. The equivalent values of φ' and c' are then given by expressions that can be obtained from the publication of Hoek *et al.* (2002).

It is worth mentioning that Data Mining techniques were also applied in order to obtain new models for the

strength parameters, namely *c*' and φ' in granite formations (Miranda, 2007).

3.4. Selection of design geomechanical parameters

In the adoption of shear strength parameter values taken for design purposes are selected rather than determined. The selection of deformability and strength parameters for foundation on rock requires mainly sound engineering judgment and experience based on the results of tests performed and on the use of empirical systems (ASCE, 1996; Wyllie, 1999).

The selection of design shear strength parameters is dependent on the site geological structure taking into consideration the discontinuities, the rock and planes of weakness.

Failure envelopes for upper and lower bounds of shear strength can be determined for the three potential types of failure surfaces, namely for intact rock, clean discontinuities and filled discontinuities. Technical Engineering and Design Guides from US Army Corps of Engineers, n. 16, describes the appropriate selection procedures (ASCE, 1996).

Using the H-B criterion, the publication from Serrano & Olalla (2007), published at the 11th ISRM Congress, presents a synthesis of the applicability of this criterion and the identification of the applicable parameters. The most important hypotheses of the developed work are related to the theory of plasticity.

The deformational response of a deep rock foundation must be assessed in order to estimate the building settlements and the implications in the neighboring structures. Assumptions for deformation and settlements are normally based on the hypothesis that the rock mass behaves as a continuum and the expressions used are based in the theory of elasticity. Therefore, the selection of design parameters normally involves the selection of Poisson's ratio and deformability modulus. For almost all rock masses, Poisson's ratio varies between 0.1 and 0.35 and as a rule, lower values correspond to poorer quality rock masses. The selection of an adequate deformability modulus is most important in order to make reliable predictions of deformations and settlements of deep rock foundations.

4. Design Processes of Rock-Socketed Shafts

4.1. Introduction

The design of deep rock foundations includes the typical bearing capacity and settlement analyses. These analyses are performed to establish the capacity of the foundation to support the loads without bearing failure and without excessive deformations or settlements. Available data should be obtained during design, including geomechanical information of the rock mass as discontinuities, faults and other features; depth of overburden; ground water condition and load conditions (Kulhawy & Carter, 1992a,b; ASCE, 1996).

Rock-socketed shafts or caissons are constructed in drill holes extending below the building to depths where sound rock masses can sustain the applied loads. They are used where structural loads are substantial and allowable settlements small as is the case for tall buildings. Drilled shafts are usually oriented vertically and used to support compressive loads.

Drilled shafts may be installed or drilled through the soil to end bearing on rock or drilled to some depth into the rock. Drilling large diameter holes in rock is expensive and consequently the length and the diameter of the socket should be minimized. An investigation of the ground conditions should be carried out in order to identify the geological features. When dealing with karstic formations it is necessary to perform borings in order to find the optimum depth and plan location of shafts. In these cases the approach for foundation design has to accommodate a high degree of uncertainty.

It is important to obtain information about the compressive strength of the rock in order to determine the bearing capacity and the deformability modulus used to predict settlements. Rock mass deformability modulus can be determined using dilatometer or rock pressuremeter tests, correlated if possible with more accurate *in situ* tests like the PLT. Information on ground water is essential for determination of the construction conditions.

Socketed shafts can be designed to support the loads in side-wall shear comprising adhesion or skin friction on the socket wall; or end bearing on the material below the tip; or a combination of both. When the shaft is drilled some depth into sound rock, a combination of side-wall shear and end bearing can be assumed. Foundation capacity depends on the shaft materials, the geotechnical material where the shaft is founded, the loading and the construction method. The mechanism of load transfer and settlement of the shaft is illustrated in Fig. 10. In the figure, k_s and k_b represent, respectively, the shaft resistance and the bearing end. The support provided in side-wall shear Q_s and end bearing Q_b are equal to the product of the displacement and the applicable spring stiffness ($Q_s = k_s\delta_s$ and $Q_b = k_b\delta_b$).

In the third case presented in Fig. 10, the shaft has been drilled through material with low modulus to end bearing on material with higher deformability modulus. It means that k_b is much greater than k_s. Much of the displacement will occur due to elastic shortening of the shaft and relatively small amount due to deflection of the material below the shaft base. Most of the load is carried in end bearing for this configuration (Wyllie, 1999).

The behavior of rock socketed shafts has been studied through laboratory and *in situ* tests and by using numerical models. The results of this investigation work have shown that the following factors have important influence on the

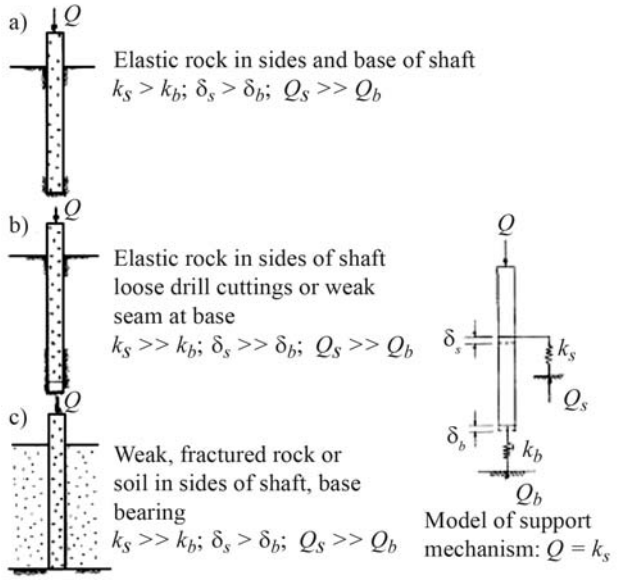

Figure 10 - Simplified support mechanism for socketed shafts (adapted from Wyllie, 1999).

load capacity and settlement of the shaft (Kulhawy & Carter, 1992a; Wyllie, 1999):

• *Socket geometry* - The geometry of a rock socket is defined by the length to diameter ratio and has significant effect on the load capacity of the shaft. As the ratio increases, the load carried in end bearing diminishes and progressively more load is carried in side-wall shear.

• *Rock mass modulus* - The shear stress on the sidewalls of a socket is partially dependent on the normal stress acting at the rock mass surface and the magnitude of normal stress related to the stiffness of the surrounding rock formation.

• *Rock mass strength* - The shear strength on the side-walls of the socket and the bearing capacity of the rock mass below the shaft base are related to the strength of the rock mass. Shear strength behavior is different of rough and smooth sockets.

• *End of socket* - If it is assumed that load is carried in end bearing, it is fundamental to assure that the end of socket should be cleaned, because a low modulus material in the socket base will allow considerable displacements of the shaft to take place before end bearing is mobilized. The use of TV cameras can be of assistance in performing the inspection.

• *Rock mass layering* - Layers of weak rock in the socket and at the base may influence the load bearing capacity of the shaft.

• *Creep* - In formations subject to creep, the influence of time can have a great importance. The proportion of the load carried in end loading varied from 15 to 20% of the load at the top of the shaft. While the strain gauges along the shaft showed increasing load with time, the load at the base showed minimal increase.

To predict the strength properties of the rock mass, the use of empirical systems is nowadays very important and the H-B criterion is usually applied. A synthesis of the numerical analysis related to the ultimate bearing capacity and pullout strength force for deep and shallow foundations using the H-B criterion was recently presented (Serrano & Olalla, 2007). The theory associated to the ultimate bearing capacity evaluation at the tip of a pile embedded in rock is also presented in the referenced publication. Figure 11 shows a simplified scheme of the plastic flow net at the tip of a shaft.

The design and construction of deep foundations can be carried out as represented in Fig. 12. Design starts with site investigation and ground parameter evaluation varying in quality and quantity according to the importance and complexity of the project.

Possible foundation schemes are identified based on the results of the investigation, load requirements and local practice. All possible schemes are evaluated relying on load tests. The objectives of these tests are to verify that the shafts' response to loading are in agreement with anticipated response, and to ensure that the ultimate capacities are not less than the calculated ones.

The Osterberg Load tests, also referred to O-cell tests, are commonly used in conjunction with drilled shafts and are often a cost-effective alternative to static load tests. They can be placed anywhere within the shaft (Figs. 13 and 14). In all applications the cell expands to apply equal loads to the portions of the foundation element above and below the cell. Recent history shows a significant increase in maximum loads applied during these tests (England & Cheesman, 2005).

4.2. Design values

Rock socketed shafts can be designed to carry compressive loads in side-wall shear only, end bearing only or combination of both. Important factors affecting the design

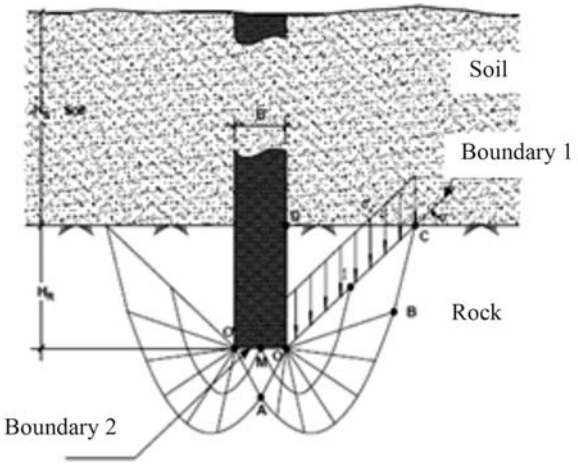

Figure 11 - Simplified scheme of the plastic flow net at the tip of a shaft (Serrano & Olalla, 2007).

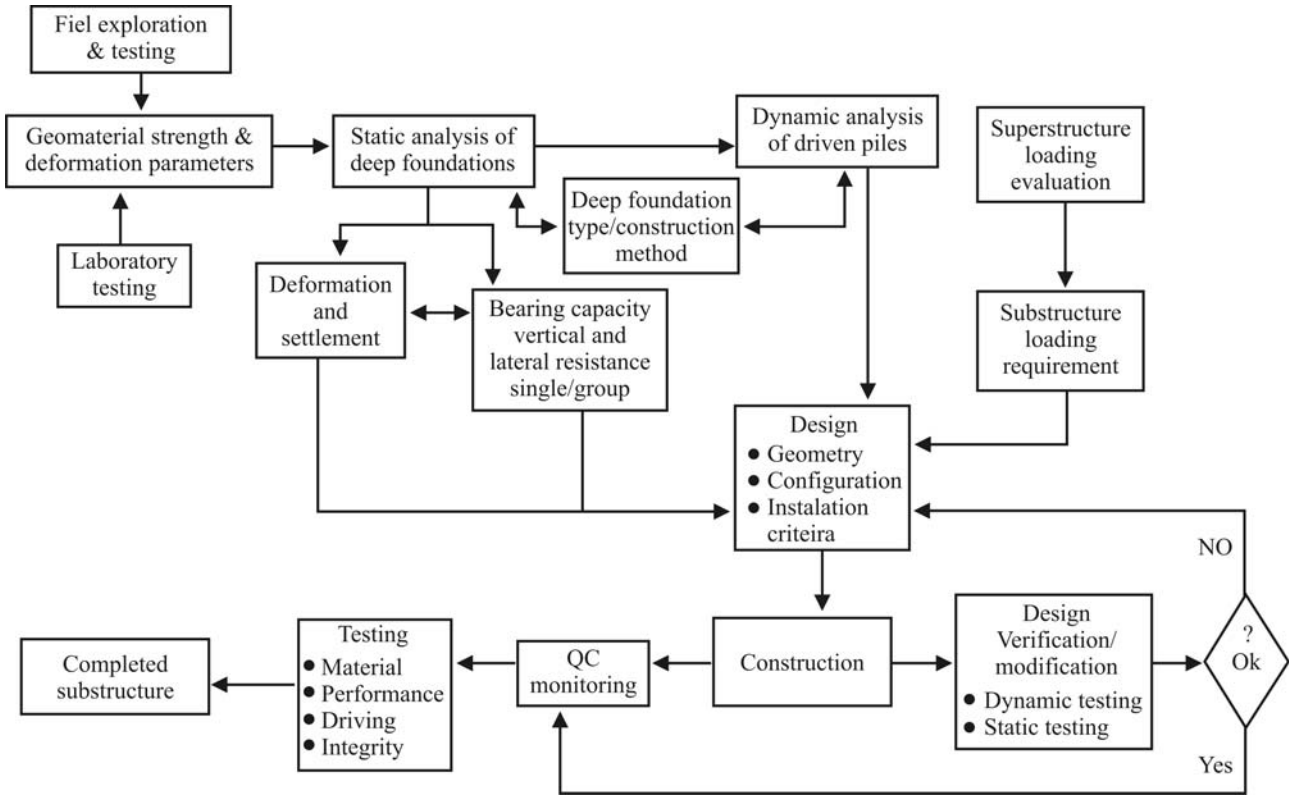

Figure 12 - Design and construction process for deep foundations (Paikowsky, 2004).

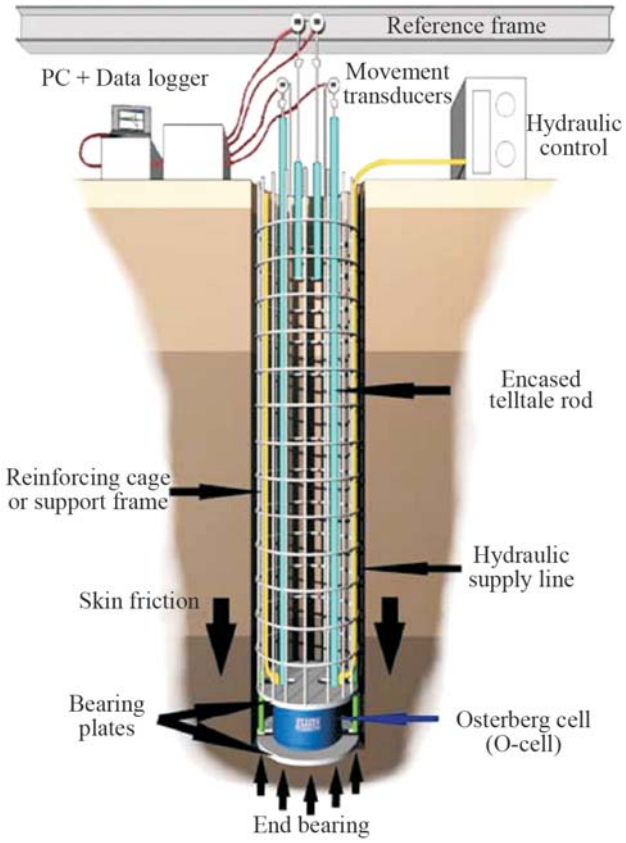

Figure 13 - Bi-direccional test schematic (England & Chessman, 2005).

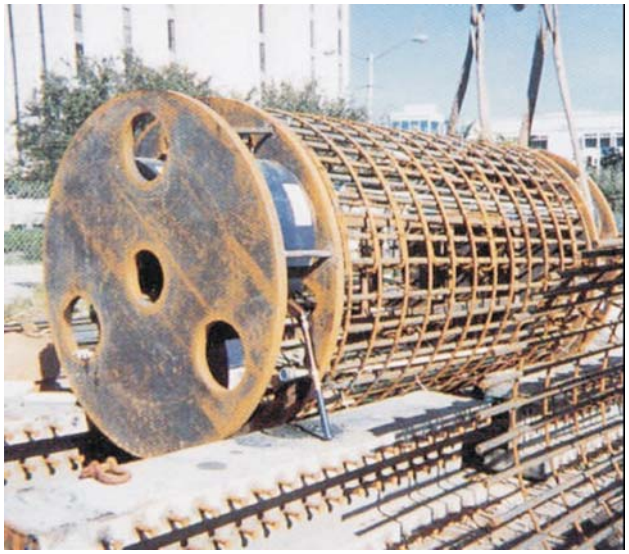

Figure 14 - High capacity testing with multiple O-cell (England & Chessman, 2005).

are strength, degree of fracturing, E (deformability modulus) of rock mass, condition of walls and base of the socket, and the geometry of the socket.

The load capacity calculation in side-wall shear assumes that shear stress is uniformly distributed in the socket walls and the capacity is given by:

$$Q = \tau_a \pi B L \quad (6)$$

where Q is the total applied load, τ_a is the allowable side-wall shear stress, B and L are the diameter and length of socket, respectively. The diameter is usually determined by the available drilling equipment and the length is selected in order to have a side-wall shear stress not greater than the allowable shear stress and to ensure that the design settlement is not exceeded.

Based on the publication of Wyllie (1999), some design values are presented:

• For clean sockets, with side-wall undulations between 1 and 10 mm deep and less than 10 mm wide:

$$\tau_a = \frac{0.6(\sigma_{u(r)})^{0.5}}{FS} \quad (7)$$

or

$$\tau_a = \frac{(\beta\sigma_{u(r)})}{FS} \quad (8)$$

where $\sigma_{u(r)}$ is the uniaxial compressive strength of the rock for smooth and grooved sockets, FS is safety factor and β the adhesion factor ($\tau/\sigma_{u(r)}$) as defined in a graphic presented in the previous referred publication.

• For clean sockets, with side-wall undulations greater than 10 mm deep and 10 mm wide:

$$\tau_a = \frac{0.75(\sigma_{u(r)})^{0.5}}{FS} \quad (9)$$

Values for the adhesion factor β may be available from test shafts. The factor of safety FS relates the ultimate to the allowable shear resistance. A $FS = 2.5$ relates the ultimate to the allowable stress values in these test shafts. If the rock mass is closely fractured, the values of τ_a should be reduced.

An end-bearing socket may fracture a cone of rock beneath the end of the shaft which will result in excessive settlement. Experience has shown that shafts have been loaded to base pressures as high as three or more the compressive strength of rock without collapse. Test results showed that allowable load capacity Q_a with a FS of about two to three equals:

$$Q_a = \sigma_{u(r)} \frac{\pi B^2}{4} \quad (10)$$

For conditions where the rock below the shaft contains sub-horizontal seams infilled with lower strength material the end-bearing capacity is reduced and the equation is:

$$Q_a = K' \omega \sigma_{u(r)} \quad (11)$$

where

$$K' = \frac{3 + \frac{S}{B}}{10\left(1 + 300\frac{t}{s}\right)^{1/2}} \quad (12)$$

ω is a depth factor and is equal to

$$\omega = 1 + \frac{0.4L}{B}$$

for $\omega < 3$. s is the spacing of the seams and t is the thickness of the filled.

4.3. Settlements

Also based on the publication of Wyllie (1999) some expressions for settlement predictions are presented.

For settlements calculation of socketed shafts, a 3-stage process can be developed with the increasing load as follows:

• Deformation starts at shaft with elastic compression and with elastic shear strain at the rock-grout interface. The deformation is small and the major portion of the load is carried in side-wall shear.

• Slippage starts and increasing load is transferred to the pillar base.

• The rock-concrete bond is broken and increasing load is carried in end bearing.

Different socket conditions exist depending on the site geology and construction method (Fig. 15).

The general equation for settlements of socketed shafts that support the load in shear-wall resistance at the surface of a semi-elastic half space is:

$$\delta = \frac{QI}{BE_{m(s)}} \quad (13)$$

$E_{m(s)}$ is the modulus of deformation of rock mass in the shaft and I is a settlement influence factor given by Fig. 16. In this figure R is the ratio between E_c and $E_{m(s)}$. E_c is the deformability modulus of the shaft. Values of rock mass have been back-analyzed and the following equation was proposed:

$$E_{m(s)} = 110\sqrt{\sigma_{u(r)}} \quad (14)$$

It should be noted that the described influence factors assume that the socket is fully bonded from the rock surface. However, influence factors could be reduced where the shaft is recessed below the surface.

When the load is entirely supported in end bearing, the settlement is calculated in a similar manner of a footing near the ground surface. Using reduction factors given by Fig. 17, the equation for settlements of an end bearing shaft is:

$$\delta = \frac{4Q}{\pi B^2}\left[\frac{D}{E_c} + \frac{RF' C_d B(1-\nu^2)}{E_{m(b)}}\right] \quad (15)$$

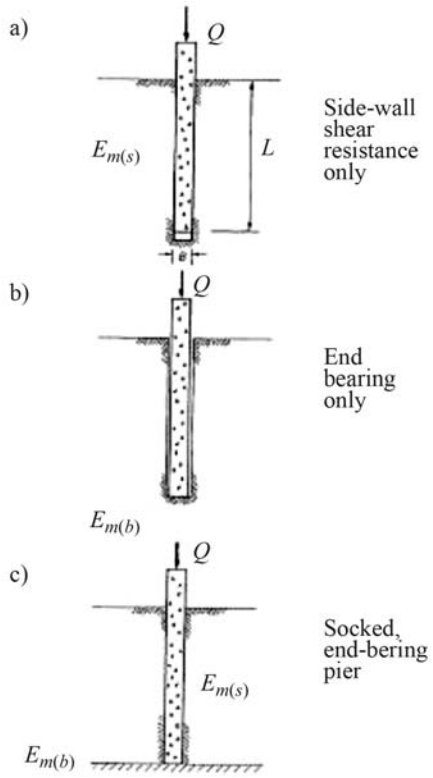

Figure 15 - Summary of calculation methods of settlements (Adapted from Wyllie, 1999).

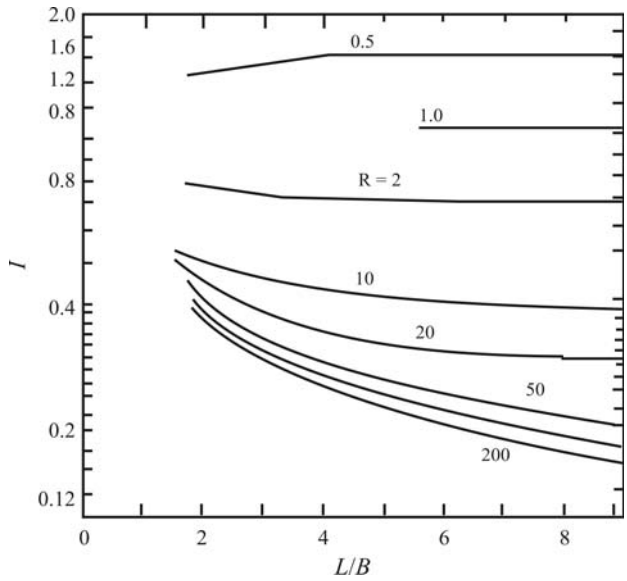

Figure 16 - Elastic settlement factors for side-wall resistance socketed shaft (Adapted from Wyllie, 1999).

where D is the depth of shaft, B the diameter of socket, RF' is a reduction factor given by Fig. 17 and C_d is the shape and rigidity factor as referred in Table 8. Q is the foundation load and $E_{m(b)}$ is the deformation modulus of the rock mass in the shaft base.

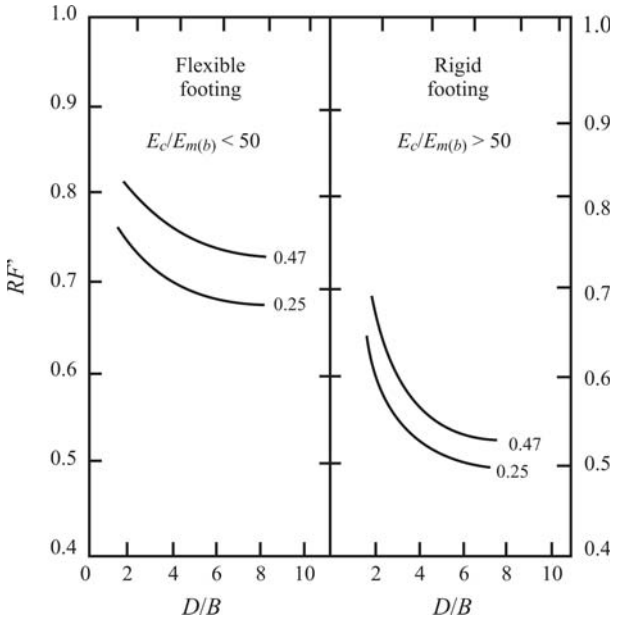

Figure 17 - Reduction factors for calculation of settlement of end bearing sockets (Adapted from Wyllie, 1999).

Table 8 - Shape and rigidity factors C_d.

Shape	Center	Corner	Average
Circle	1.00	0.64	0.64
Circle (rigid)	0.79	0.79	0.79
Square	1.12	0.56	0.76
Square (rigid)	0.99	0.99	0.99
Rectangle: length/width			
1.5	1.36	0.67	0.97
2	1.52	0.76	1.12
3	1.78	0.88	1.35
5	2.10	1.05	1.68
10	2.53	1.26	2.12
100	4.00	2.00	3.60
1000	5.47	2.75	5.03
10000	6.90	3.50	6.50

Also the settlement can be calculated for a mixed situation of the load being carried out by end bearing behavior and along side walls.

5. Analysis of Tall Buildings Foundations

5.1. Empire State Building

The Empire State Building was the tallest building in the world when completed in 1931 as referenced in Table 1. It remained as the world's tallest building until 1972, when the twin towers of the World Trade Center were completed. The most significant statistic of the Empire State was its status as a tall skyscraper and also the extraordinary speed with which it was planned and constructed (Willis, 1998). In real-

ity, six months after setting the first structural column, the steel frame topped off at the eighty-sixth floor. The full building was finished in eleven months, in March 1931.

Figure 18 presents the plan of the ground floor, with a plan area of about 7,796 m^2, and shows a schematic of the foundation layout using 210 shafts.

Based on the publication of Willis (1998), some information about the Empire State is presented. Manhattan bedrock is mostly granite and schist and therefore is capable of supporting high loads. At the site of Empire State Building it ranged to about 23 m below grade, with concrete shafts to transmit loads from the base of the steel columns to the bedrock. Tops of these shafts were reinforced with grillages of steel beams.

Foundation excavation started on January 22, 1930 and finished on March 17, 1931. The excavated material consisted of 6,881 m^3 of soil and 13,303 m^3 of rock material. The concrete poured into 210 shafts totalled about 2,863 m^3. Taking into consideration that shafts have a depth between 9.1 and 12.2 m, an average diameter of about 1.2 m was estimated for each shaft. The excavated rock was soft and it was necessary to go deep in order to get the hard rock necessary to pass tests required by New York City.

The shaft excavation started on February 12, 1930 and first shaft holes satisfied hard rock bottom criteria imposed by City Inspectors and were filled with concrete on February 24.

The first steel columns were set on April 7, 1930 and the building was completely finished on March 1, 1931. The entire project was conceived and successfully executed within twenty-one months.

The theory presented in Section 4 of this article was used to estimate settlements that might have occurred during construction of the Empire State Building.

Considering expression (14), and taking into consideration the average UCS value of 161.4 MPa obtained for granites presented in Table 4, the modulus of deformability $E_{m(s)}$ obtained for the foundation is equal to about 1.4 GPa. This corresponds to a bad geomechanical quality rock mass, with low values for RMR and Q geomechanical indexes. Consequently using this deformability modulus the corresponding RMR value was calculated. According to

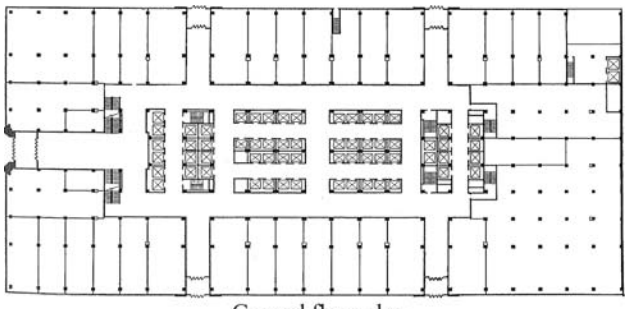

Figure 18 - Empire State Building ground floor plan (Willis, 1998).

our experience and based also on Data Mining applications performed in rock formations (Miranda, 2007), the expressions proposed by Serafim and Pereira (1983) and Hoek and Brown (1997) gave good results in terms of $E_{m(s)}$ calculation. The Serafim and Pereira (1983) expression was adopted due to our experience. The expression takes into consideration in situ tests performed in several countries in Europe, South America and Africa.

Applying that expression, and for the value of E previously calculated, a value of $RMR = 16$ was obtained. This value is low and corresponds to a class V rock mass according to the RMR empirical system. A higher value of RMR was also adopted ($RMR = 30$) as more representative of the granite Empire State foundation. The value of E obtained was then equal to 3.2 GPa. These two values (1.4 and 3.2 GPa) were adopted for the analysis of the Empire State foundation.

Considering the hypothesis that all the loads at the foundation are entirely supported by the end bearing of the shafts, Eq. (15) permits estimation of the maximum expected settlement.

A deformability modulus of 50 GPa for E_c was adopted for the composite columns of steel and concrete, and a factor C_d of 0.64 corresponding to the average between center and edge for a circle was chosen. For Poisson's ratio the value of 0.2 was adopted. The diameter of the socket shaft was considered $B = 1.2$ m and for the depth of the shaft an average value of $D = 10.7$ m was taken.

The ratio of the modulus E_c to the modulus of the rock mass below the base, for both situations, is equal to 35.7 and 15.6, *i.e.* less than 50, so it can be assumed that the base of the shaft act as a flexible footing. The reduction factor RF' for a flexible footing on a rock with a Poisson's ratio of 0.2 and a depth to diameter ratio, $D/B = 10.7/1.2 = 8.9$, is about 0.65.

Consequently the settlements are equal to:

1st hypothesis ($E = 1.4$ GPa),

$$\delta = 0.0491Q \quad (16)$$

2nd hypothesis ($E = 3.2$ GPa),

$$\delta = 0.0322Q \quad (17)$$

being settlement in cm and Q the applied force per shaft expressed in MN.

The evaluation of Q was obtained applying the International Building Code (IBC, 2006). Live load adopted for hotels and residential areas are equal to 1.915 kPa and for offices are 2.394 kPa. Due to the absence of information, two values were considered for the dead load, equal to and double that of the live load.

The floor area is about 7,800 m^2 and the total number of concrete and steel caissons is 210. It was assumed the existence of 86 floors plus an upper tower. The values for Q in

MN were estimated and presented in Table 9, as well the corresponding settlements.

For the performed simulations, the maximum value obtained for the settlements was 1.3 cm, with a minimum of 0.5 cm. Of course these values could be smaller because the load supported in both side-wall shear of the shafts is not considered. However the calculated settlements do not take creep into consideration.

5.2. Chicago buildings

In this section special reference is made to the IBM building in Chicago and to the Chicago Spire now under construction.

Table 9 - Predicted values for forces and settlements at the foundation.

Calculation	Pressure (kPa)	Q (MN)	Settlement (cm)
C1 (E = 1.4 GPa)	4.309	14.2	0.7
C2 (E = 3.2 GPa)	4.309	14.2	0.5
C3 (E = 1.4 GPa)	7.962	26.2	1.3
C4 (E = 3.2 GPa)	7.962	26.2	0.8

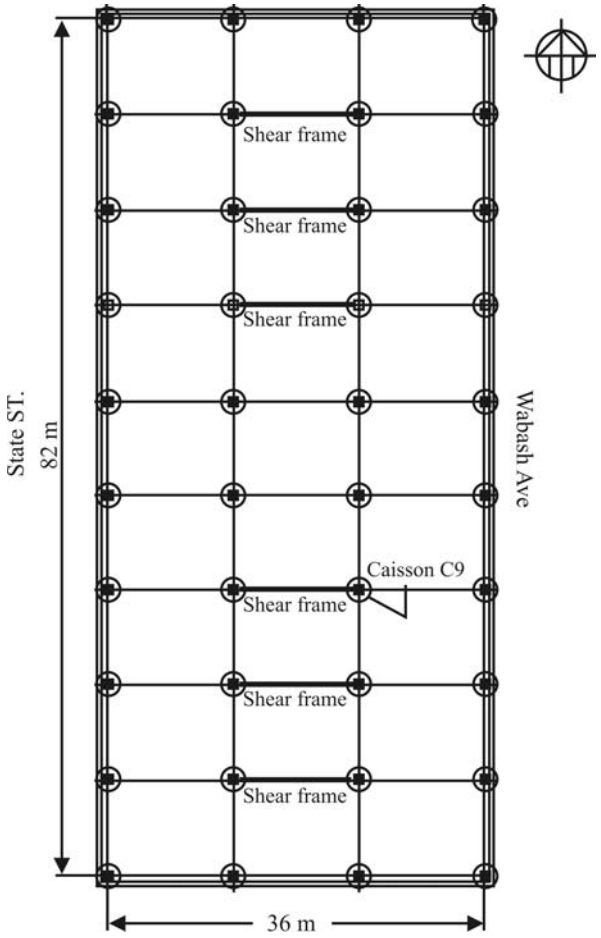

Figure 19 - Caisson and column plan of IBM Chicago Building (Task Force on Foundations, 1972).

The IBM building has 52 stories and rises about 204 m and is supported by 40 caissons. Caisson C9 is instrumented as shown in Fig. 19. The sound rock is represented by a limestone rock formation. The design bearing capacity of the sound limestone was about 12 MPa and the shaft was extended around 0.9 m into sound rock.

The Chicago Committee on High Rise Buildings, formed in 1969, initiated a research for the economic design, construction and maintenance of tall buildings. The Committee decided to analyse the caissons of the IBM building at the time under construction. A new code was proposed recognizing that the steel shell strengthens the caisson allowing an increase the permissible concrete stress (Task Force on Foundations, 1972).

The main purpose of the project was to evaluate the caisson design criteria adopted in 1970, and to check the structure performance to other design criteria used in the Chicago Code. The list of criteria studied was namely related to gravity loads, wind loads, base plate pressure, caisson shell and rock pressure (Task Force on Foundations, 1972).

A borehole was drilled through the caisson and 2.1 m in the bedrock. For the concrete an average values of 41 GPa were obtained for the modulus of elasticity and 40.5 MPa for the compressive strength. Analysis of monitored data was performed in detail once the loading started. The last readings were taken at the end of December, 1971. After that the building was completed and partially occupied.

The evaluation of test measurements was described by the following comments (Task Force on Foundations, 1972):

• Computations were performed considering 65% of dead load and 35% of live load. During construction the loads computed by strain measurements were in good agreement with the design dead load.

• The monitored results show that the total load carried by the steel shell can be evaluated using the theory of elasticity and indicated a rapid transfer of the load from the concrete to the steel shell. Rock sockets should be designed as composite columns

• The study of wind effect was performed during a period in 1971. The magnitude of the load caused by wind agrees reasonably well with the design hypothesis.

• Horizontal tensile stresses were measured in the upper part of the caisson, but compressive stresses are measured in the lower part of the caisson. The effect of Poisson ratio's which causes tensile stresses is counteracted by the horizontal soil pressures.

• Strain meter measurements near the bottom of the steel shell indicate no decrease in steel stress, but indicate a decrease in stress on the concrete. Some of the load is being carried in shear between rock and caisson perimeter.

• It was recommended to increase the ultimate bearing pressure of the rock of about 50% above greater than the

previous value, leading to adoption of the value of 28.7 MPa.

The case of the Chicago Spire foundation will provide 34 concrete and steel caissons. A 31.7 m diameter and 23.8 m deep cofferdam will be excavated to create a dry work environment. The caissons will be drilled 36.6 m deep into the bedrock to support the 150-story building's structure. The cofferdam, bathtube-like structure, will serve as the foundation for the building core. The works are taking place near the docks belonging to Chicago Line Cruises (Figs. 5 and 6).

From its many extraordinary features, the Spire will have the world's longest continuous elevator running about 610 m from the underground garage to the 150th floor. The construction of the underground phase will be finished in 2008. The excavations started in June, 2007 (Fig. 20).

The Chicago Spire will be the tallest all-residential structure, will have the most slender profile, and will bear on one of the most tall-building bases ever built. The tower will stand on 34 rock-socketed caissons at a design load of 25.8 MPa, 50% higher than city code allows for large-diameter shafts, and verified to 57.5 MPa using Osterberg cells. The Spire's 33.5 m deep foundations received a special permit in the 2007 summer (Hampton, 2007).

The shafts are arranged in two rings, one 33.5 m in diameter to support a concrete, tapered core that would sit seven levels below grade, and another, 64 m diameter ring of 14 caissons that would hold seven steel perimeter megacolumns at grade. The superstructure contract requires building the core from the bottom up, while excavating a parking garage from the top down.

The Chicago building code section for rock caissons is based on an empirical formula that allows incremental increases in end bearing pressure for each foot of embedment into solid rock, to a maximum value of 19.1 MPa. For maximum design efficiency, a code variance was sought and approved to increase bearing pressure to 23.9 MPa with confirmation load testing by a load test on a 2.4 m rock caisson and in the study conducted by the Chicago Committee on High Rise Buildings (Task Force on Foundations, 1972). The Osterberg cell at the bottom of the rock socket was loaded to its maximum capacity of 23.9 MPa and negligible movement was recorded. The city code also permits higher allowable stress in the rock caisson concrete, provided that it is confined in permanent steel casing of a certain wall thickness.

Figure 20 - Beginning of excavations for the Chicago Spire foundation.

Chicago has surficially some of the youngest geology in the country. The whole Great Lakes landscape was "wiped clean" and replaced with till during the ice age; the most recent glaciation was only 10,000 or so years ago. The rock is about 30.5 m below the surface and usually has a weathered and broken horizon with fractures and clay seams. The unweathered limestone beneath is sound and fairly hard, in the range of 69 to 138 MPa.

The floor area of the Spire is about 278,700 m^2 with 34 rock-socketed caissons, the existence of 150 floors plus the existence of more underground. Therefore expected settlements could be significant (Hampton, 2007).

6. Final Remarks

The study performed for deep rock foundations lead to the following brief comments:

• For skyscrapers suitable bearing surfaces often occur at considerable depths in rock formations. In these cases, socketed shafts or caissons would be required.

• The worldwide tendency is towards living in megacities. To accommodate the population the construction of skyscrapers is expected to continue as a major trend, which is corroborated by the impressive tall buildings now in construction.

• The selection of deformability and strength parameters of rock foundation requires sound engineering judgment and experience based on results of tests and the use of empirical systems. Artificial intelligence techniques should be applied in order to develop new geomechanical models.

• A description of design methodologies for deep rock foundations was presented. Better predictions required the use of refined three-dimensional numerical models.

• The analysis of foundations of tall buildings in the USA was performed, considering buildings in New York and Chicago. The existing geomechanical information was scarce. However, reasonable conclusions can be reached.

Acknowledgments

Appreciation is expressed to Lachel Felice & Associates, USA, which supported the preparation of this work.

References

ASCE (1996) Rock Foundations (Technical Engineering and Design Guides as adapted from US Army Corps of Engineers, n. 16). American Society of Civil Engineers, New York, 129 pp.

Babendererde, S.; Hoek, E.; Marinos, P. & Cardoso, S. (2006) Characterization of granite and the underground construction in Metro do Porto. Matos, A.C.; Sousa, L.R.; Kleberger, J. & Pinto, P.L. (eds) Geotechnical Risk in Rock Tunnels, Francis & Taylor, London, pp. 41-51.

Baguelin, F.; Jézéquel, J. & Shields, D. (1978) The Pressuremeter and Foundation Engineering. Trans Tech Publications, Cluasthal, 617 pp.

Barton, N. (2000) TBM Tunnelling in Jointed and Faulted Rock. Balkema, Rotterdam, 172 pp.

Barton, N.; Lost, F.; Lien, R. &Lunde, J. (1980) Application of the Q-system in design decision concerning dimensions and appropriate support for underground installations. Bergman, M. (ed.) Subsurface Space 2, Pergamon, New York, pp. 553-561.

Barton, N. & Quadros, E. (2002) Engineering and hydraulics in jointed rock masses. Symposium EUROCK 2002 - Course A, Funchal.

Bieniawski, Z. (1975) Case studies: Prediction of rock mass behavior by the geomechanical classification. Proc. 2nd Australia-New Zealand Conference Geomechanics, Brisbane, pp. 36-41.

Bieniawski, Z. (1978) Determining rock mass deformability, experience from case histories. Int. Journal of Rock Mechanics and Mining Science, n. 15, p. 237-247.

Bieniawski, Z. (1989) Engineering Rock Mass Classifications. John Wiley & Sons, New York, 251 pp.

Binder, G. (2006) Tall Buildings of Europe, the Middle East and Africa. Images Publishing Group, Victoria, 240 pp.

Cafofo, P. (2006) Projecto hidroeléctrico de Socorridos (Socorridos hydroelectrical project). Final project in Geotechnics, University of Minho, Guimarães, 90 pp.

Carter, T.; Diederichs, M. & Carvalho, J. (2007) A unified procedure for Hoek-Brown prediction of strength and post yield behaviour for rock masses at the extreme ends of the rock competency scale. Proc. 11th ISRM Congress, Lisbon, pp. 161-164.

Carvalho, J. (2004) Estimation of rock mass modulus. Personal communication.

Carvalho, J.; Carter, T. & Diederichs, M. (2007) An approach for prediction of strength and post yield behaviour for rock masses of low intact strength. Proc. 1st Canada USA Rock Symposium, Vancouver, 8 pp.

Christensen, B. (2005) Taipei 101 tower causing earthquakes? www.technovelgy.com.

DFI (2008) Case Foundation Tackles Spire Site. Deep Foundations Institute, Hawthorne, pp. 75.

Diederichs, M. & Kaiser, P. (1999) Stability of large excavations in laminated hard rockmasses: The Voussoir analogue revisited. Int. Journal of Rock Mechanics and Mining Science, v. 36, p. 97-117.

Douglas, K. (2002) The Shear Strength of Rock Masses. PhD Thesis, School of Civil and Environmental Engineering, The University of New South Wales, Sydney, 284 pp.

England, M. & Cheesman, P.F. (2005) Recent experiences with bi-direccional static load testing. http://www.docstoc.com/docs/22682470/recent-experiences-with-bi-directional-static-load-testing 9 pp.

Hampton, H. (2007) Pier pressure may make or break Spire. ENR Engineering News - Record, December. http://www.loadtest.com/loadtest-usa/sidelogs/profiles/ENR1207.pdf.

Hoek, E. (2006) Practical Rock Engineering. www.rocscience.com.

Hoek, E. & Brown, E.T. (1997) Practical estimates of rock mass strength. Int. Journal of Rock Mechanics and Mining Science, n. 34, p. 1165-1186.

Hoek, E.; Carranza-Torres, C. & Corkum, B. (2002) Hoek-Brown failure criterion - 2002 edition. Proc. 5th NARMS Symposium, Toronto, pp. 267-273.

Hoek, E. & Diederichs, M. (2006) Empirical estimation of rock mass modulus. Int. Journal of Rock Mechanics and Mining Science, n. 43, p. 203-215.

IBC (2006) International building code. Code and Commentary, 2 v. http://www.iccsafe.org/Pages/default.aspx.

Judd, W.R. (1969) Statistical Methods to Compile and Correlate Rock Properties and Preliminary Results. Purdue University, Lafayette, 109 pp.

Kulhawy, F. & Carter, J. (1992a) Settlement and bearing capacity of foundations on rock masses. Bell, FG (ed) Eng. in Rock Masses. Butherworth-Heinemann, Oxford, pp. 231-245.

Kulhawy, F. & Carter, J. (1992b) Socketed foundations in rock masses. Bell, FG (ed) Eng. in Rock Masses. Butherworth-Heinemann, Oxford, pp. 509-529.

Kulhawy, F. & Goodman, R.E. (1987) Foundations in rock. In: Ground Engineer's Reference Book. Butterworth, London, pp. 1-13.

Lima, C.; Resende, M.; Plasencia, N. & Esteves, C. (2002) Venda Nova II hydroelectric scheme powerhouse geotechnics and design. ISRM News Journal, v. 7:2, p. 37-41.

Marinos, P. & Hoek, E. (2005) Estimating the geotechnical properties of heterogeneous rock masses such asch. Bulletin Engineering Geology and Environment, n. 60, p. 85-92.

Miranda, T. (2003) Contribuição para o Cálculo de Parâmetros Geomecânicos na Modelação de Estruturas Subterrâneas em Formações Graníticas (Contribution to the Calculation of Geomechanical Parameters for Underground Structures Modeling in Granite Formations). MSc Thesis, Civil Engineering Department University of Minho, Guimarães, 186 pp.

Miranda, T. (2007) Geomechanical Parameters Evaluation in Underground Structures. Artificial Intelligence,

Bayesian Probabilities and Inverse Methods. PhD Thesis, University of Minho, Guimarães, 291 pp.

Miranda, T.; Sousa, L.R. & Correia, A.G. (2008) Bayesian framework for the deformability modulus updating in an underground structure. Proc. 42th U.S. Rock Mechanics Symposium, San Francisco, 7 p CD-ROM).

Mitri, H.; Edrissi, R. & Henning, J. (1994) Finite element modeling of cable bolted stopes in hard rock underground mines. SME Annual Meeting, Albuquerque, pp. 14-17.

Nicholson, G. & Bieniawski, Z. (1997) A non-linear deformation modulus based on rock mass classification. Int. Journal of Mining and Geology Engineering, n. 8, p. 181-202.

Paikowsky, S. (2004) Load and resistance factor design (LRFD) for deep foundations. National Cooperative Highway Research Program, Report 507, Washington, 74 pp.

Plasencia, N. (2003) Underground Works - Aspects of the Engineering Geology Contribution and Design. MSc Thesis, Technical University of Lisbon, Lisbon (in Portuguese).

Post, N. (2008a) Building sector needs reeducation. ENR Engineering News - Record, March, pp. 10-12. http://enr.ecnext.com/coms2/article_nebuar080312a.

Post, N. (2008b) 650-plus meters skyward, crews are already. Out of this world. ENR Engineering News - Record, May, pp. 26-33. http://enr.ecnext.com/coms2/article_febiar080430-1.

Read, S.; Richards, L. & Perrin, N. (1999) Applicability of the Hoek-Brown failure criterion to New Zeland greywacke rocks. Proc. 9th ISRM Congress, Paris, pp. 655-660.

Reina, P. (2006) Final height on 'on deck' tallest tower shrouded in secrecy. ENR Engineering News - Record, June. http://enr.construction.com/features/_covers/2006/06-default1.asp.

Rocha, M. (1971) Rock Mechanics (in Portuguese). LNEC, Lisbon, 276 pp.

Serafim, J.L. & Pereira, J. (1983) Considerations of the geomechanics classification of Bieniawski. Proc. of the Int. Symposium of Engineering Geology on Underground Construction, Lisbon, pp. II.33-II.42.

Serrano, A. & Olalla, C. (2007) Bearing capacity of shallow and deep foundations in rock with the Hoek and Brown failure criteria. Proc. 11th ISRM Congress, Lisbon, v. 3, pp. 1379-1392.

Singh, S. (1997) Time Dependent Modulus of Rocks in Tunnels. MSc Thesis, Civil Engineering Department, University of Roorkee, 153 pp.

Sonmez, H.; Gokceoglu, C. & Ulusay, R. (2004) Indirect determination of the modulus of deformation of rock masses based on the GSI system. Int. Journal of Rock Mechanics and Mining Science, n. 41, p. 849-857.

Sousa, L.R.; Leitão, N.S. & Monteiro, G. (1999) Observed behavior of the structures for the power increase of the Miranda hydroelectric project. Proc. 9th ISRM Congress, Paris, pp. 1603-1612.

Sousa, L.R.; Nakamura, A.; Yoshida, H.; Yamaguchi, Y.; Kawasaki, M. & Satoh, H. (1997) Evaluation of the deformability of rock masses for dam foundations. Analysis of deformability investigation results in heterogeneous bedrock. Technical Memorandum n. 3514, Public Works Research Institute, Tsukuba, 45 pp.

Stephens, S. (2004) Imagining Ground Zero. Official and Unofficial Proposals for the World Trade Center Site. McGraw-Hill Construction, NewYork, 224 pp.

STS (2006) Viewpoint 5, STS Consultants.

Task Force on Foundations (1972) Strain measurements in rock-socketed caisson. Chicago Committee on High Rise Buildings, Report n. 3, Chicago, 50 pp.

Verman, M.; Singh, B.; Viladkar, M. & Jethwa, J. (1997) Effect of tunnel depth on modulus of deformation of rock mass. Rock Mech. Rock Engng., v. 30:3, p. 121-127.

Willis, C. (1998) Building the Empire State. Skyscraper Museum, New York, 190 pp.

Wyllie, D. (1999) Foundations on Rock. E & FN Spon, London, 401 pp.

Yufin, S.; Lamonina, E. & Postolskaya, O. (2007) Estimating of strength and deformation parameters of jointed rock masses. Proc. 5th Int. Work. on Applications of Computational Mechanics in Geotechnical Engineering, Guimarães, pp. 3-15.

List of Symbols and Acronyms

α: Modulus reduction factor

β: adhesion factor

γ: volumic weight

δ: settlement

σ_1', σ_3': Maximum and minimum effective principal stresses

σ_c: uniaxial compressive strength

σ'_{cm}: rock mass strength

$\sigma_{t,mass}$: tensile strength of the rock mass

$\sigma_{u(r)}$: unconfined compressive strength for smooth and grooved sockets

φ': effective friction angle

τ_a: Allowable side-wall shear stress

B, *L*: diameter and length of the socket, respectively

c': effective cohesion

C_d: Shape and rigidity factor

D: disturbance factor of the GSI system

E: deformability modulus of the rock mass

E_c: deformability modulus of concrete

E_i: deformability modulus of the intact rock

$E_{m(s)}$: deformability modulus of the rock mass in the shaft

$E_{m(b)}$: deformability modulus of the rock mass in the base

H: depth
I: settlement influence factor
m_b, s, a: strength parameters of the Hoek and Brown strength criterion for the rock mass
m_i: strength parameter of the Hoek and Brown strength criterion for the intact rock
k_s, k_b: shaft and end bearing resistance of piles
Q: applied load to the pile
Q_a: allowable load capacity of the pile
RF': reduction factor
S: spacing of the seams
t: thickness of the filled
ASCE: American Society of Civil Engineers
DFI: Deep Foundations Institute
DM: Data Mining
FS: Safety factor
GSI: Geological Strength Index
H-B: Hoek and Brown
ISRM: International Society of Rock Mechanics
LFJ: Large Flat Jack test
PLT: Plate Load Test
Q: Q system index value
RMR: Rock Mass Rating
SFJ: Small Flat jack test
STS: STS Consultants
STT: LNEC Strain Tensor Tube
UCS: Uniaxial compressive strength